February 2023| Volume 02 | Issue 01 | Pages 09-14

Future Energy
Open Access Journal
ISSN 2832-0328

Journal homepage: https://fupubco.com/fuen

https://doi.org/10.55670/fpll.fuen.2.1.2

Future Publishing LLC

Article

Theoretical analysis of the performance and optimization of indirect flat evaporative coolers

Hamidreza Asemi[1], Rahim Zahedi[2]*, Sareh Daneshgar[3]

[1]Faculty of Engineering, Science and Research Branch, Islamic Azad University, Tehran, Iran
[2]Department of Renewable energy and Environmental Engineering, University of Tehran, Tehran, Iran
[3]Faculty of Electrical Engineering, Iran University of Science and Technology, Tehran, Iran

ARTICLE INFO

Article history:
Received 13 July 2022
Received in revised form
16 August 2022
Accepted 22 August 2022

Keywords:
Indirect Evaporative Cooling,
Exergy, Optimization

*Corresponding author
Email address:
Rahimzahedi@ut.ac.ir

DOI: 10.55670/fpll.fuen.2.1.2

ABSTRACT

External-cooling indirect evaporative coolers with different configurations and working air sources are incomprehensively analyzed and compared so far. This paper investigates the mechanism and theory of operation of indirect flat-panel evaporative coolers based on X-analysis. Then, based on the second law of thermodynamics analysis, the entropy production rate of the flat-plate heat exchanger of the cooler is calculated. As a result of this analysis, the optimal energy efficiency-evaporation efficiency and cooling capacity values are presented in terms of effective parameters in the design.

1. Introduction

One of the most common methods used to cool environments is the passage of hot air over wet surfaces at low temperatures, called "evaporative cooling." This method is considered compared to mechanical (compression) cooling systems due to its cheaper and non-use harmful refrigerant in the ozone layer [1]. An essential drawback of this type of cooling is the lack of proper control of ambient humidity. This form is produced by the indirect evaporative cooling method to a large extent, and cooling with the desired quality is prepared. Mode of operation as shown in Figure 1, indirect evaporative coolers have two primary and secondary airflows. The initial air has no contact with moisture and enters the desired environment after cooling. Suppose the secondary air is in direct contact with the water film. In that case, this action causes the water film to evaporate and the transformer plates to cool down, eventually removing heat from the primary air. The mixture of these two breaths of air provides favorable conditions for the environment. Rawabawale and Sapali [2] analytically evaluated the influence of size variation of the cooling tower on exergy loss and found that the cooling tower with a larger length than height yields smaller exergy loss with higher thermal efficiency. Kiyaninia et al. [3] experimentally and theoretically investigated the exergoeconomic performance of a solar photovoltaic-based direct evaporative air-cooling system. The results showed that for an inlet air with a temperature of 30^{o}C and relative humidity of 30%, the maximum system exergy efficiency was obtained at about 20%. Martineza et al. [4] and Nada et al. [5] studied the energy and exergy performance of different wet pad materials of evaporative coolers through experiments and found that the exergy efficiency was between 70% and 94% under different pad thicknesses. This research comparatively analyzes the energy and exergy performance of indirect flat evaporative coolers on the basis of a verified numerical model and experimental correlation.

2. Thermal analysis

The control volume is considered for thermal analysis of the cooler according to Figure 2. It is worth mentioning that the analysis of the mass heat transfer process of this type of air conditioner is complex. Therefore, in the thermal study, it is necessary to consider hypotheses to do the calculations quickly. Hypotheses are:

- Lewis number: 1 = Le
- Mass heat transfer coefficients are assumed to be constant.

- The effect of mass heat transfer between secondary air droplets is considered to be negligible.
- Saturation enthalpy changes with humid secondary air temperature are linear.
- The plates are considered completely wet.
- Heat transfer to the environment is negligible.

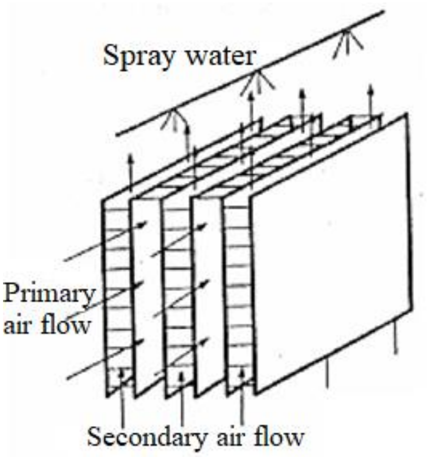

Figure 1. Isometric view of indirect evaporation cooler

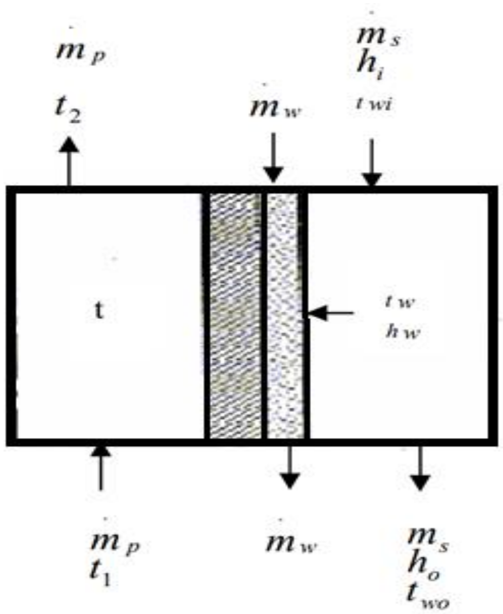

Figure 2. Control volume of an indirect evaporative cooler

2.1 Energy balance for primary air

According to Figure 2, the primary air loses its heat significantly, so:

$$U_0(t - t_w) = \dot{m}_P c_P \, dt \tag{1}$$

As a result, after integration, the number of primary air units using X-theory is as follows [6].

$$(NTU)_p = \frac{U_0 A}{m_P c_P} = -\ln\left(\frac{t_2 - t_1}{t_1 - t_w}\right) \tag{2}$$

The initial air impact factor will be as follows.

$$\varepsilon_P = 1 - exp(NTU)_\rho = \frac{t_1 - t_2}{t_1 - t_w} \tag{3}$$

2.2 Energy balance for secondary air

In Figure 2, a differential element from the air contact surface shows a wet surface. Thermal balance for the earth element from [7]:

$$h_D(h_w - h)\, dA = \dot{m}_s \, dh \tag{4}$$

By integrating equation (5)

$$(NTU)_s = \frac{h_D A}{\dot{m}_s} = \frac{h_D c_P A}{\dot{m}_s c_P} = -\ln\left(\frac{h_0 - h_w}{h_0 - h_i}\right) \tag{5}$$

After arranging the above equation, the coefficient of the effect of the secondary air is as follows:

$$\varepsilon_s = 1 - exp(-NTU)_s = \frac{h_i - h_0}{h_i - h_w} \tag{6}$$

According to the linear proportion of changes in the enthalpy of humid air with the ratio of temperatures [8]:

$$c_{wb} = \frac{h_0 - h_i}{tw_0 - tw_i} \tag{7}$$

C_{wb} is the specific saturation temperature of equation (7) as follows.

$$\varepsilon_s = 1 - exp(-NTU)_s = \frac{tw_0 - tw_i}{tw_i - tw} \tag{8}$$

Assuming 1 = Le (i.e., assuming that the rate of penetration of the rate of heat transfer and mass diffusion are the same at the contact surface of air-water):

$$Le^{2/3} = \frac{h_C}{h_D C_\rho} \rightarrow h_C = C_\rho h_D \tag{9}$$

With replacement (9) in (5):

$$(NTU)_s = \frac{h_c A}{\dot{m}_s c_P} = -\ln\left(\frac{tw_0 - tw}{tw_i - tw}\right) \tag{10}$$

2.3. Energy balance between the primary and secondary air

By defining the coefficient of cooling effect in indirect evaporative coolers [9]:

$$\varepsilon_s = \frac{t_1 - t_2}{t_1 - tw_i} \tag{11}$$

The energy balance equation between the primary and secondary air will follow:

$$\dot{m}_p c_P (t_1 - t_2) = \dot{m}_s (h_O - h_i) \tag{12}$$

Incidentally, according to equation (7)

$$t_2 = t_1 - \frac{c_{max}}{c_{min}}(tw_0 - tw_i) \tag{13}$$

While C_{min} and C_{max} are:

$$c_{min} = \dot{m}_p c_P \tag{14}$$

$$c_{max} = \dot{m}_s c_{wb} \tag{15}$$

By placing equation (13) in equation (2):

$$\varepsilon_P = \frac{c_{max}}{c_{min}}\left(\frac{tw_0 - tw_i}{t_1 - tw}\right) \tag{16}$$

By placing equation (6) in equation (5), water temperature

$$t_w = \frac{\varepsilon_s\left(\frac{c_{max}}{c_{min}}\right)+\varepsilon_P+t_1}{\varepsilon_s\left(\frac{c_{max}}{c_{min}}\right)+\varepsilon_P} \tag{17}$$

By placing equation (17) in equation (2), the coefficient of the cooling effect of the cooler is:

$$\varepsilon_C = \frac{1}{\frac{1}{\varepsilon_P}+\frac{1}{\varepsilon_S}\left(\frac{\dot m_P c_P}{\dot m_S c_{wb}}\right)} \tag{18}$$

In addition, to calculate the heat transfer coefficients of the primary and secondary air passages and the sticky surface, respectively [10] are:

$$Nu = 0.023 {Re_{Dh}}^{4/5} Pr^{1/2} \quad Re > 2300 \tag{19}$$

$$Nu = 7.54 \quad Re \le 2300 \tag{20}$$

Where: $Re_{Dh} = \frac{4\dot m}{\Pi D \mu}$, $D_h = 2b$

2.4. Calculate the drop in air flux by multiplying the capacity of the air conditioner

The pressure drop of the whole system due to local friction drops is calculated according to the following equations [11].

$$\Delta P_f = f\frac{L}{D_h}\frac{v^2\rho}{2} \tag{21}$$

$$\Delta P_l = \sum K\frac{v^2\rho}{2} \tag{22}$$

$$\Delta P_t = \Delta P_f + \Delta P_l \tag{23}$$

As a result, the required power of the device blower, assuming η_m =1, is [12]:

$$w = \frac{\dot m_P \Delta P_P}{\eta_P} + \frac{\dot m_s \Delta P_s}{\eta_s} \tag{24}$$

2.5. Calculating the energy efficiency ratio

The energy efficiency ratio of EER is equal to

$$EER = \frac{Q_c}{w} \tag{25}$$

Where Q_c is the cooling capacity of the indirect air conditioner can be calculated from the following equation.

$$Q_c = \dot m_p c_P (t_1 - t_2) \tag{26}$$

2.6. Analysis of the second law for indirect plate evaporative coolers

There are several evaluation criteria for the optimal operating conditions of thermal systems. One of the most reliable criteria is the second law analysis or exergy analysis. Figure 2 shows that an indirect plate air conditioner is like a plate heat exchanger with the opposite flow for secondary airflow and cross-flow for primary air. In order to obtain a statement to calculate the initial airflow exergy rate, we assume that the surface temperature of the plates is constant throughout the length of the plate, which is a reasonable assumption for this type of cooler. The rate of production of primary exergies of such plates is as follows, which includes two parts: output and output [13, 14].

$$\left(e_{t,p}\right)_{in} = R_a t_1 \ln\left(1+1.6\right)\omega_o \tag{27}$$

$$\left(e_{t,p}\right)_{out} = c_P t_0\left(\frac{t_2}{t_0} - 1 - \ln\frac{t_2}{t_0}\right) + R_a t_0 \ln\left(1 - \frac{\Delta P}{P_0}\right) + R_a t_o \ln\left(1+1.6\right)\omega_o \tag{28}$$

Moreover, entropy production for secondary air is in equations (29) and (30). In addition to heat transfer and friction, it also has the mass transfer term due to evaporation, which consists of input and output.

$$\left(e_{t,s}\right)_{in} = \left(c_P + \omega c_{Pv}\right)t_0\left(\frac{t_{Wi}}{t_0} - 1 - \ln\frac{t_{Wi}}{t_0}\right) + (1 + 1.6\omega_o)R_a t_0 \ln\left(\frac{P}{P_0}\right) + R_a t_0\left[(1+1.6\omega_o)\ln\frac{1+1.6\omega_o}{1+1.6\omega} + 1.6\omega_o \ln\frac{\omega}{\omega_0}\ \right] \tag{29}$$

$$\left(e_{t,s}\right)_{out} = \left(c_P + \omega_{out} c_{P,v}\right)t_0\left(\frac{t_{Wo}}{t_0} - 1 - \ln\frac{t_{Wo}}{t_0}\right) + (1 + 1.6\omega_{out})\, R_a t_0 \ln\left(1 - \frac{\Delta P}{P_0}\right) + R_a t_0\left[(1+1.6\omega_{out})\ln\frac{1+1.6\omega_o}{1+1.6\omega_{out}} + 1.6\omega_{out} \ln\frac{\omega_{out}}{\omega_o}\ \right] \tag{30}$$

As a result, the total entropy production rate is calculated as follows:

$$s_{gen} = \frac{1}{T_0}\left\{\left[\dot m_P e_{tp} + \dot m_s e_{ts}\right]_{in} - \left[\dot m_P e_{tp} + \dot m_s e_{ts}\right]_{out}\right\} \tag{31}$$

Based on the entropy production equations (27 to 31), the design method of indirect coolers mentioned in the first part of the article, the functional relationship of the total entropy production rate is as follows:

$$\dot s_{gen} = f\left(\dot m_p, \dot m_s, L, w\right) \tag{32}$$

3. Results and Discussion

A computer code has been prepared to calculate the design values such as the temperature of the air leaving the air conditioner, the energy efficiency ratio, and to observe the effect of effective parameters such as plate length and mass flow rate on the EER according to Figure 3. Figures 3 and 4 result from these calculations. As shown in Figure 4, the initial outlet air temperature of the T2 model was compared with the experimental reference results [4]. The difference between the modeling results and the experimental results is about 3%, and this difference is due to ignoring the effects of environmental parameters in modeling. Figure 5 compares the cooling effect of X with the experimental results [4]. After designing the system according to equations (27) to (32), the entropy produced by the system is investigated. It is evident that the system, based on the design conditions, is faced with limitations in selecting the values of W and L. Due to these limitations, the mentioned values must be considered in a specific range. The variables are examined by keeping the other parameters constant on the entropy production rate of the system, and finally, the optimal values of the system design are obtained. It is worth noting that the optimization of design variables by the exergy method (the second law of thermodynamics) is not economically optimal for systems. Therefore, in practice, in order to optimize the systems, both thermo economic studies should be done.

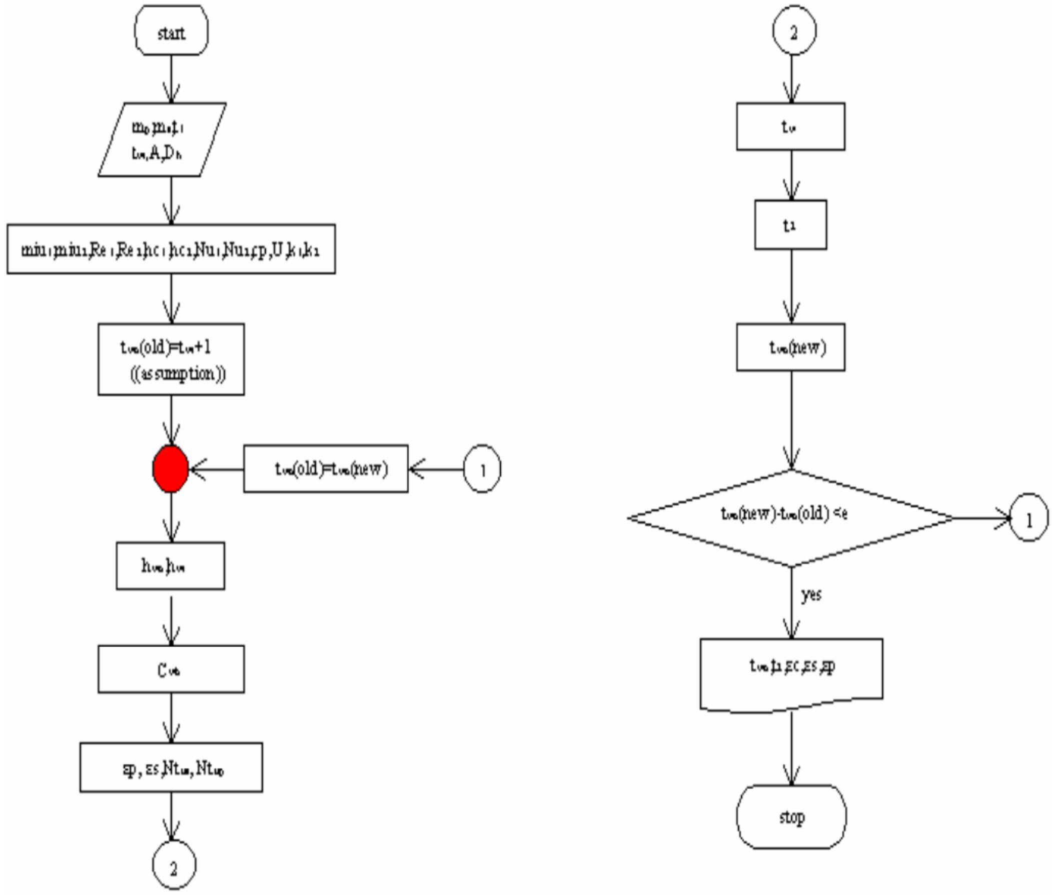

Figure 3. Flowchart design of direct evaporative coolers

Figure 6 shows the entropy production rate in terms of the secondary air flow rate changes at a constant value of the primary airflow rate. The design shows that the maximum and minimum point distance values are minimal. Figure 7 shows the entropy production rate of initial airflow. As shown in this figure, the maximum and minimum entropy production points are not within the design range. This trend indicates the low sensitivity of the entropy production rate to the initial air flow rate.

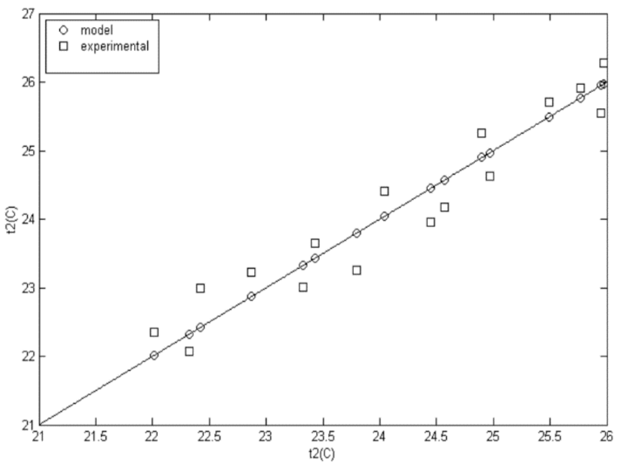

Figure 4. Comparison of the initial air outlet temperature of the model with experimental results

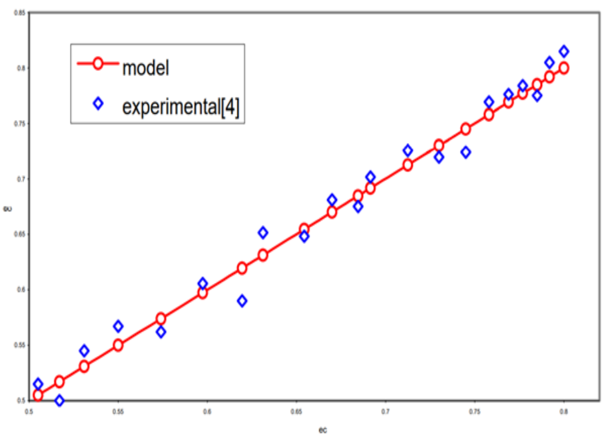

Figure 5. Comparison of the cooling coefficient of the model air conditioner with the experimental results

Figures 8 and Figure 9 show the entropy production rate in secondary air discharge in different primary discharges and the entropy production rate in secondary air discharge in different primary discharges, respectively. As can be seen, at a certa in amount of primary or secondary air flow rate, the minimum entropy production can be achieved by selecting another reasonable flow rate. Figure 10 also shows the entropy production rate in terms of plate length. It is observed that the longer the plate lengths are selected in this type of short coolers, the more the entropy production rate increases. As a result, the length of the pages should be selected by the primary and secondary discharges for maximum efficiency.

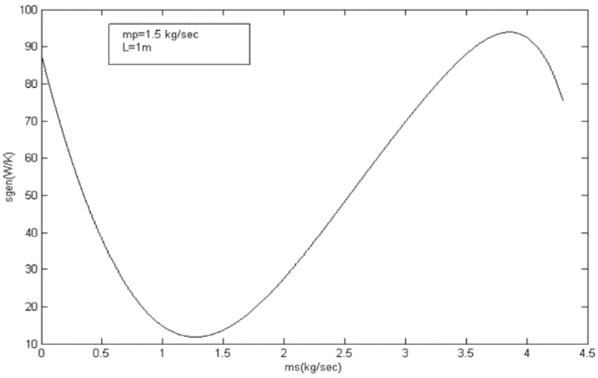

Figure 6. Entropy production rate in terms of secondary air flow

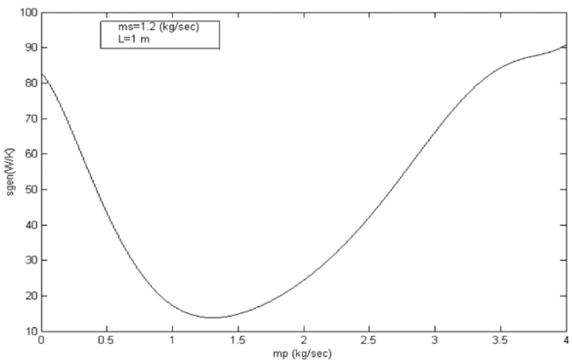

Figure 7. Entropy production rate in terms of initial air flow

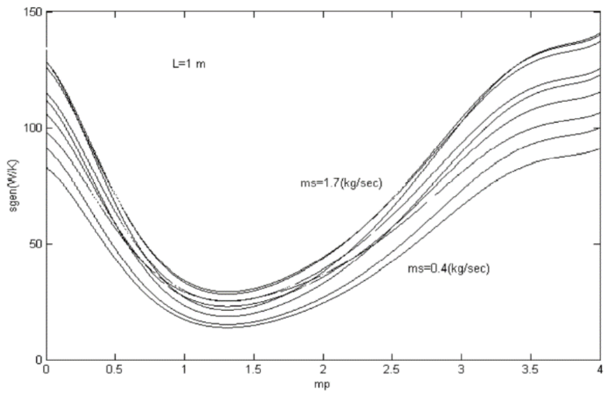

Figure 8. Entropy production rate in terms of primary air discharge in secondary discharges

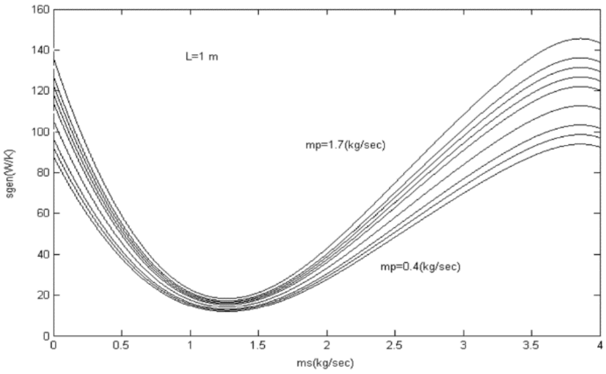

Figure 9. Entropy production rate in terms of secondary air flow in primary flows

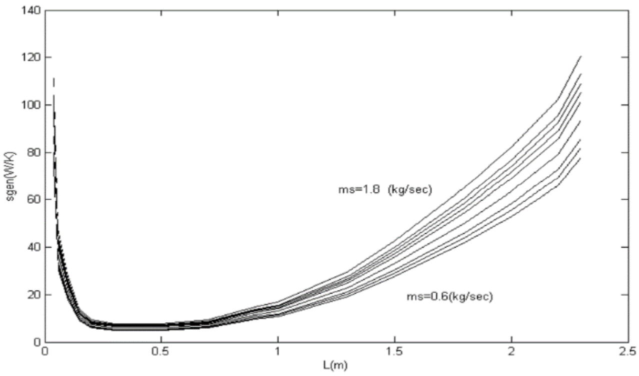

Figure 10. Entropy production rate in terms of plate length in secondary discharges

4. Conclusions

In this study, the energy and exergy performance of cooling indirect flat evaporative coolers and direct evaporative coolers are compared and analyzed on the basis of the developed mathematical model. The main conclusions are given as follows:

1) Indirect evaporative coolers have better performance than direct evaporative coolers in dry areas.

2) Exergy analysis is an excellent tool to optimize the parameters affecting the performance of indirect evaporators. The increased fresh air flowrate reduces the cooling efficiency and exergy efficiency of all evaporative coolers.

Ethical issue

The authors are aware of and comply with best practices in publication ethics, specifically with regard to authorship (avoidance of guest authorship), dual submission, manipulation of figures, competing interests, and compliance with policies on research ethics. The authors adhere to publication requirements that the submitted work is original and has not been published elsewhere in any language.

Data availability statement

Data sharing is not applicable to this article as no datasets were generated or analyzed during the current study.

Conflict of interest

The authors declare no potential conflict of interest.

Abbreviations and Greek symbols

A	Effective heat transfer surface (m^2)
B	The distance between the two cooler plates (m)
C_{max}	Maximum heat transfer capacity(W/^{o}C)
C_{min}	Minimum heat transfer capacity(W/^{o}C)
C_p	Specific heat capacity to air (KJ/Kg ^{o}C)
C_{pv}	Specific heat capacity of water vapor (KJ/Kg ^{o}C)
D_h	Hydraulic diameter (m)
$e_{t,p}$	Primary air exergy (W/KgK)
$e_{t,s}$	Secondary air exergy (W/KgK)
h_i	Enthalpy of secondary air inlet (KJ/Kg)
h_o	Enthalpy of secondary air outlet (KJ/Kg)
h_w	Enthalpy of air saturation at the common air and water level (KJ/Kg)
K	Local drop coefficient
L	The length of the plates of indirect evaporators (m)
Le	Louis Number
$\dot{m}_a$	Air mass flow (Kg/s)
$\dot{m}_p$	Primary air flow (Kg/s)
$\dot{m}_s$	Secondary air flow (Kg/s)
EER	Energy efficiency ratio
f	Friction coefficient
h_c	Conduction heat transfer coefficient (W/m^{2o}C)
h_D	Mass transfer coefficient (Kg/m^2s)
Nu	Nusselt number
ΔP_f	Pressure drop due to friction (Pa)
ΔP_l	Local pressure drop (Pa)
ΔP_p	Initial pressure drop
ΔP_s	Secondary pressure drop
Pr	Prandt number
Re	Reynolds number
S_{gen}	Production entropy
t_1	Dry bubble temperature of the primary air inlet
t_2	Dry bubble temperature of the primary air outlet
t_{wi}	Wet bubble temperature of secondary air inlet
t_{wo}	Wet bubble temperature of secondary air outlet
t_w	Saturation temperature of the joint surface of air and water
t_o	Ambient temperature
$\dot{m}_w$	Mass flow of water
NTU_p	Number of primary air transfer units
NTU_s	Number of secondary air transmission units
U_0	The total heat transfer coefficient between the primary air and the common surface of the secondary air of water
ε_C	Cooler effect coefficient
ε_p	Primary air impact coefficient
ε_s	Secondary air impact coefficient
ρ	Air density
η_p	Fan efficiency of the first part
η_s	Secondary fan efficiency
μ	Adhesion coefficient
ω_{out}	Humidity for secondary exhaust air
ω_0	Humidity for the environment

References

[1] Y. Yang, G. Cui, and C. Q. Lan, "Developments in evaporative cooling and enhanced evaporative cooling-A review," Renewable and Sustainable Energy Reviews, vol. 113, p. 109230, 2019.

[2] N. Rawabawale, "Exergy analysis ofthe cross current cooling tower," Journal of Thermal Engineering, vol. 6, no. 4, pp. 499-510, 2020.

[3] A. Kiyaninia, H. Karimi, and V. M. Avargani, "Exergoeconomic analysis of a solar photovoltaic-based direct evaporative air-cooling system," Solar Energy, vol. 193, pp. 253-266, 2019.

[4] P. MARTíNEZ, J. Ruiz, P. Martínez, A. Kaiser, and M. Lucas, "Experimental study of the energy and exergy performance of a plastic mesh evaporative pad used in air conditioning applications," Applied Thermal Engineering, vol. 138, pp. 675-685, 2018.

[5] S. Nada, A. Fouda, M. Mahmoud, and H. Elattar, "Experimental investigation of energy and exergy performance of a direct evaporative cooler using a new pad type," Energy and Buildings, vol. 203, p. 109449, 2019.

[6] Z. Duan et al., "Indirect evaporative cooling: Past, present and future potentials," Renewable and sustainable energy reviews, vol. 16, no. 9, pp. 6823-6850, 2012.

[7] R. Zahedi, S. Daneshgar, M. A. N. Seraji, and H. Asemi, "Modeling and interpretation of geomagnetic data related to geothermal sources, Northwest of Delijan," Renewable Energy, 2022.

[8] C. Guo, Q. Liu, B. Zheng, Y. You, and Y. Li, "Development of model based on condensation area ratio and effect on heat transfer capacity of indirect evaporative cooling," Applied Thermal Engineering, vol. 164, p. 114557, 2020.

[9] R. Zahedi, A. Shaghaghi, M. T. Tahooneh, and A. Ahmadi, "Numerical simulation of combustion of sulfide-biomass concentrate ingredients and contaminants in copper furnace smelting," Future Energy, vol. 2, no. 1, 2023.

[10] H. Yang, W. Shi, Y. Chen, and Y. Min, "Research development of indirect evaporative cooling technology: An updated review," Renewable and Sustainable Energy Reviews, vol. 145, p. 111082, 2021.

[11] J. Wu et al., "Investigation of heat transfer and pressure drop of CO2 two-phase flow in a horizontal minichannel," International Journal of Heat and Mass Transfer, vol. 54, no. 9-10, pp. 2154-2162, 2011.

[12] S. Suryawanshi, T. M. Chordia, N. Nenwani, H. Bawaskar, and S. Yambal, "Efficient technique of air-conditioning," in Proceedings of the world congress on engineering, 2011, vol. 3, pp. 2036-2041.

[13] U. Sajjad et al., "A review of recent advances in indirect evaporative cooling technology," International Communications in Heat and Mass Transfer, vol. 122, p. 105140, 2021.

[14] S. Daneshgar and R. Zahedi, "Optimization of power and heat dual generation cycle of gas microturbines through economic, exergy and environmental analysis by bee algorithm," Energy Reports, vol. 8, pp. 1388-1396, 2022.